ARTICLE

Targeting an autocrine IL-6–SPINK1 signaling axis to suppress metastatic spread in ovarian clear cell carcinoma

Christine Mehner[1,2] · Erin Miller[2] · Alexandra Hockla[2] · Mathew Coban [2] · S. John Weroha[3] · Derek C. Radisky[2] · Evette S. Radisky [2]

Abstract

A major clinical challenge of ovarian cancer is the development of malignant ascites accompanied by widespread peritoneal metastasis. In ovarian clear cell carcinoma (OCCC), a challenging subtype of ovarian cancer, this problem is compounded by near-universal primary chemoresistance; patients with advanced stage OCCC thus lack effective therapies and face extremely poor survival rates. Here we show that tumor-cell-expressed serine protease inhibitor Kazal type 1 (SPINK1) is a key driver of OCCC progression and metastasis. Using cell culture models of human OCCC, we find that shRNA silencing of SPINK1 sensitizes tumor cells to anoikis and inhibits proliferation. Knockdown of SPINK1 in OCCC cells also profoundly suppresses peritoneal metastasis in mouse implantation models of human OCCC. We next identify a novel autocrine signaling axis in OCCC cells whereby tumor-cell-produced interleukin-6 (IL-6) regulates SPINK1 expression to stimulate a common protumorigenic gene expression pattern leading to anoikis resistance and proliferation of OCCC cells. We further demonstrate that this signaling pathway can be successfully interrupted with the IL-6Rα inhibitor tocilizumab, sensitizing cells to anoikis in vitro and reducing metastasis in vivo. These results suggest that clinical trials of IL-6 pathway inhibitors in OCCC may be warranted, and that SPINK1 might offer a candidate predictive biomarker in this population.

Introduction

Patients diagnosed with ovarian cancer face a 5-year survival rate of only 47%; this poor survival is driven by early metastatic spread, which is already present in 70% of patients at time of diagnosis [1–3]. Standard of care consists of general debulking surgery and chemotherapy with taxanes and platinum reagents. While patients with the predominant high-grade serous histotype have high initial

response rates [4], patients with ovarian clear cell carcinoma (OCCC), comprising 5–20% of patients depending on the population, more often present with chemotherapy refractory disease at time of first treatment, with only ~15% response rate [5–7]. Consequently, patients with advanced stage OCCC have the lowest overall survival rate among all ovarian cancers [8]. To improve survival, these patients are in need of a more disease-focused therapeutic approach, guided by biomarker expression and specifically directed toward the distinct molecular drivers of OCCC progression.

Early metastatic spread in ovarian cancer is enabled by development of abdominal malignant ascites, large volumes of fluid containing viable tumor cells capable of seeding metastatic lesions throughout the peritoneal cavity [2, 9]. These tumor cells survive and proliferate by avoiding cell death protocols that would normally be initiated upon loss of attachment (anoikis), thus becoming anoikis resistant [10]. The focus of our investigation was to identify a therapeutically targetable mechanistic pathway that interrupts and reverts anoikis resistance to inhibit metastasis in OCCC, building on work in which we recently demonstrated a role for the serine protease inhibitor Kazal type 1

✉ Evette S. Radisky
radisky.evette@mayo.edu

1   Mayo Clinic Graduate School of Biomedical Sciences, Rochester, MN, USA

2   Department of Cancer Biology, Mayo Clinic Comprehensive Cancer Center, Jacksonville, FL, USA

3   Division of Medical Oncology, Mayo Clinic, Rochester, MN, USA

(SPINK1) as a critical inducer of anoikis resistance in ovarian cancer [11].

Originally characterized as an inhibitor of pancreatic trypsins [12], SPINK1 is a secreted protein that can be overexpressed by several tumor types, among them OCCC [13–15]. We have shown that SPINK1 tumor staining is linked to poor patient survival in ovarian cancers including OCCC [11]. We further found, using cell culture models of high-grade serous ovarian cancer, that SPINK1 can increase tumor-cell survival under attachment-free conditions, conferring anoikis resistance through inhibition of serine proteases [11]. In the present study, we turn our attention to OCCC, implementing both cell-based and mouse transplantation models to elucidate the role of SPINK1 in tumor progression and metastasis of this poor prognosis subtype. We identify SPINK1 as a contributor to OCCC anoikis resistance, proliferation, and widespread peritoneal metastasis, and further find that SPINK1 expression in OCCC is regulated by interleukin-6 (IL-6).

IL-6 is an important cytokine that regulates pleiotropic functions in diverse tissue settings. Produced by most stromal and immune cells, it is well known for immunomodulatory functions as a mediator of the acute phase reaction, a promoter of T-cell expansion and activation, and an inducer of B-cell maturation [16]. In the tumor microenvironment, IL-6 is associated with pro-tumor phenotypes and often with poor prognosis [17]. Intriguingly, IL-6 can stimulate SPINK1 expression in cancer cells. Macrophage-conditioned medium and IL-6 were shown to upregulate expression of SPINK1 in hepatoblastoma cells [18] via an IL-6 response element within the SPINK1 promoter region [19]. Fibroblast-derived IL-6 was likewise found to upregulate SPINK1 in colorectal carcinoma cells via the canonical STAT3 pathway [20].

Notably the tumor stroma is not always the only or most significant source of IL-6. IL-6 can be produced directly by ovarian cancer cells [21, 22], particularly in OCCC [23]. Loss of tumor suppressor gene ARID1A combined with an activating mutation of the phosphoinositide 3-kinase catalytic subunit PIK3CA, both frequently mutated in OCCC, drove sustained tumor overproduction of IL-6 in a mutant mouse model of OCCC [24]. In stage I OCCC, such tumor expression of IL-6 has been associated with poorer survival [25]. OCCCs also express the IL-6 receptor complex comprised of IL-6Rα and gp130, and high IL-6R expression has also been correlated with poor patient survival in OCCC [26]. These observations suggest the potential for autocrine IL-6 signaling in OCCC, with possible consequences for malignant progression that remain to be explored.

In this study, we identify an IL-6–SPINK1 autocrine signaling axis as a driver of anoikis resistance, proliferation, and metastatic spread of OCCC, and demonstrate that this axis can be therapeutically targeted using the clinically established IL-6Rα inhibitor tocilizumab. Our results suggest that IL-6 pathway inhibitors may hold therapeutic value for OCCC, and that activation of the SPINK1–IL-6 pathway may predict response.

Results

SPINK1 promotes anoikis resistance and proliferation of OCCC cells

To determine the impact of SPINK1 on anoikis resistance in OCCC, we made use of two different OCCC cell lines, JHOC9 and JHOC5. We found that these OCCC cell lines showed strongly upregulated expression of SPINK1 relative to immortalized human ovarian surface epithelial cells and relative to the models of high-grade serous ovarian cancer, which we have studied previously [11] (Fig. S1). Notably, SPINK1 upregulation in ovarian cancer cells was independent of expression of trypsin, the natural target of SPINK1 in the pancreas, and despite high expression of SPINK1, the OCCC cell lines showed little or no expression of trypsin genes PRSS1 and PRSS2 (Fig. S2).

We subjected JHOC9 and JHOC5 cells to targeted silencing of SPINK1 using multiple independent lentiviral knockdown shRNAs (KD) or to transduction with a nontarget vector control (Fig. S3a, b). Cells were then plated on ultra-low attachment plates to induce the anoikis phenotype. For both cell lines, SPINK1 KD led to a modest but significant and reproducible reduction in survival, as detected at single time points using flow cytometry (Fig. 1a–c). These results were corroborated by time course experiments quantifying apoptotic signal in real time of cells grown under ultra-low attachment conditions. For both cell lines, this assay revealed a more striking susceptibility to anoikis of SPINK1 KD cells compared to controls within the first few hours of culture under detached conditions (Figs. 1d, e and S4). The susceptibility to anoikis of SPINK1 KD cells could be at least partially rescued by addition of recombinant SPINK1 protein to the media. These experiments suggest that tumor-cell-produced SPINK1 is an important mediator of anoikis resistance in OCCC cells, as blocking SPINK1 expression increases tumor cell death under detached conditions.

We next used a similar SPINK1 knockdown approach to evaluate potential effects on proliferation of JHOC9 and JHOC5 OCCC cells. We found that SPINK1 knockdown substantially and reproducibly decreased proliferation of both cell lines (Fig. 1f–h). Given that the process of OCCC metastasis throughout the peritoneum requires tumor cells to survive in a detached state in malignant ascites, to colonize peritoneal organs, and to proliferate, our findings of SPINK1 involvement in both anoikis resistance and
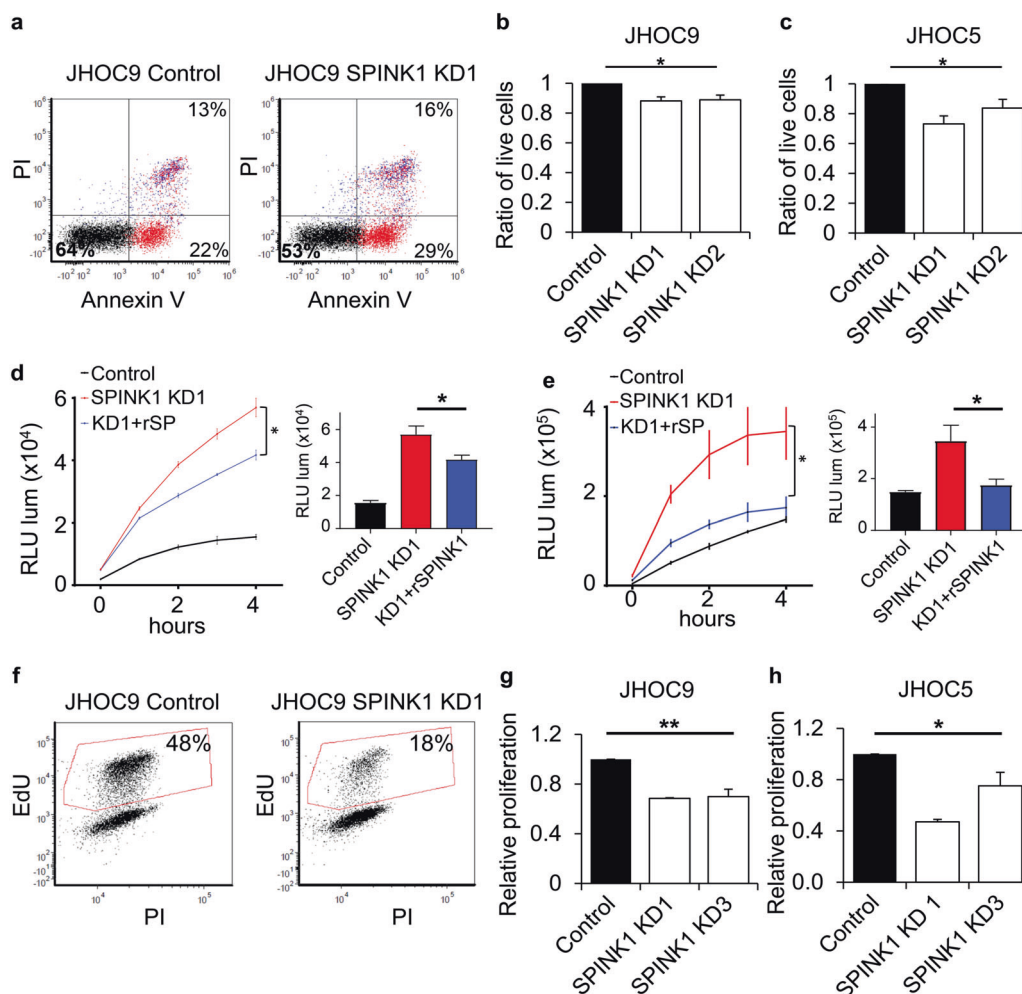
Fig. 1 SPINK1 knockdown sensitizes OCCC tumor cells to anoikis and inhibits proliferation. Significantly reduced survival of **a**, **b** JHOC9 and **c** JHOC5 cells when transduced with two different shRNA constructs targeting SPINK1 (KD1 and KD2) and grown on ultra-low attachment conditions, assessed by Annexin V and propidium iodide (PI) and quantified (**b**, **c**) by flow cytometry; data shown represent the mean and SE of three independent experiments. (One-way Anova). Time course analysis of Annexin V binding to JHOC9 (**d**) and JHOC5 (**e**) cells with knockdown of SPINK1 (red) and rescue of knockdown by addition of 500 nM recombinant SPINK1 (blue) as compared to nontarget control (black); quantification at 4 h time point. Data represent mean and SD for triplicate wells; these experiments were independently repeated with confirmatory results shown in Fig. S4. (unpaired t-test). Decreased proliferation as assessed by EdU incorporation of JHOC9 (**f**, **g**) and JHOC5 (**h**) cells with SPINK1 knockdown; data shown represent the mean and SE of two independent experiments (One-way Anova). $*p < 0.05$, $**p < 0.01$.

proliferation of OCCC cells suggest a potential role in driving tumor progression and metastatic spread.

SPINK1 promotes tumor cell survival and metastasis in mouse models of OCCC

To assess the impact of SPINK1 expression on the process of OCCC metastasis, in which shed tumor cells must survive in peritoneal ascites fluid and seed metastatic lesions, we performed intraperitoneal (IP) injections of human OCCC cell lines (JHOC9 or JHOC5), comparing cells transfected with nontarget (control) viruses or SPINK1 KD viruses (Fig. S5); both cell populations additionally expressed luciferase (Fig. S6) to enable real time in vivo

quantification of tumor burden. We found that reduction of SPINK1 expression led to significantly reduced tumor growth for both cell lines (Fig. 2a, b). At the end of the experiment, tumor growth was evident throughout the abdominal cavity in control mice, and significantly decreased with knockdown of SPINK1, for both JHOC9 (Fig. 2c, d) and JHOC5 models (Fig. 2e, f). The persistence of the knockdown was evident in reduced levels of SPINK1 protein detected by enzyme-linked immunosorbent assay (ELISA) in ascites (Fig. S7a). Analysis of ascitic fluid revealed reduced ascites volumes with SPINK1 knockdown for both cell lines (Fig. 2g, i). Evaluation of the ascitic fluid contents by immunohistochemistry (IHC) revealed extensive tumor spheroid formation in ascitic fluid in both control
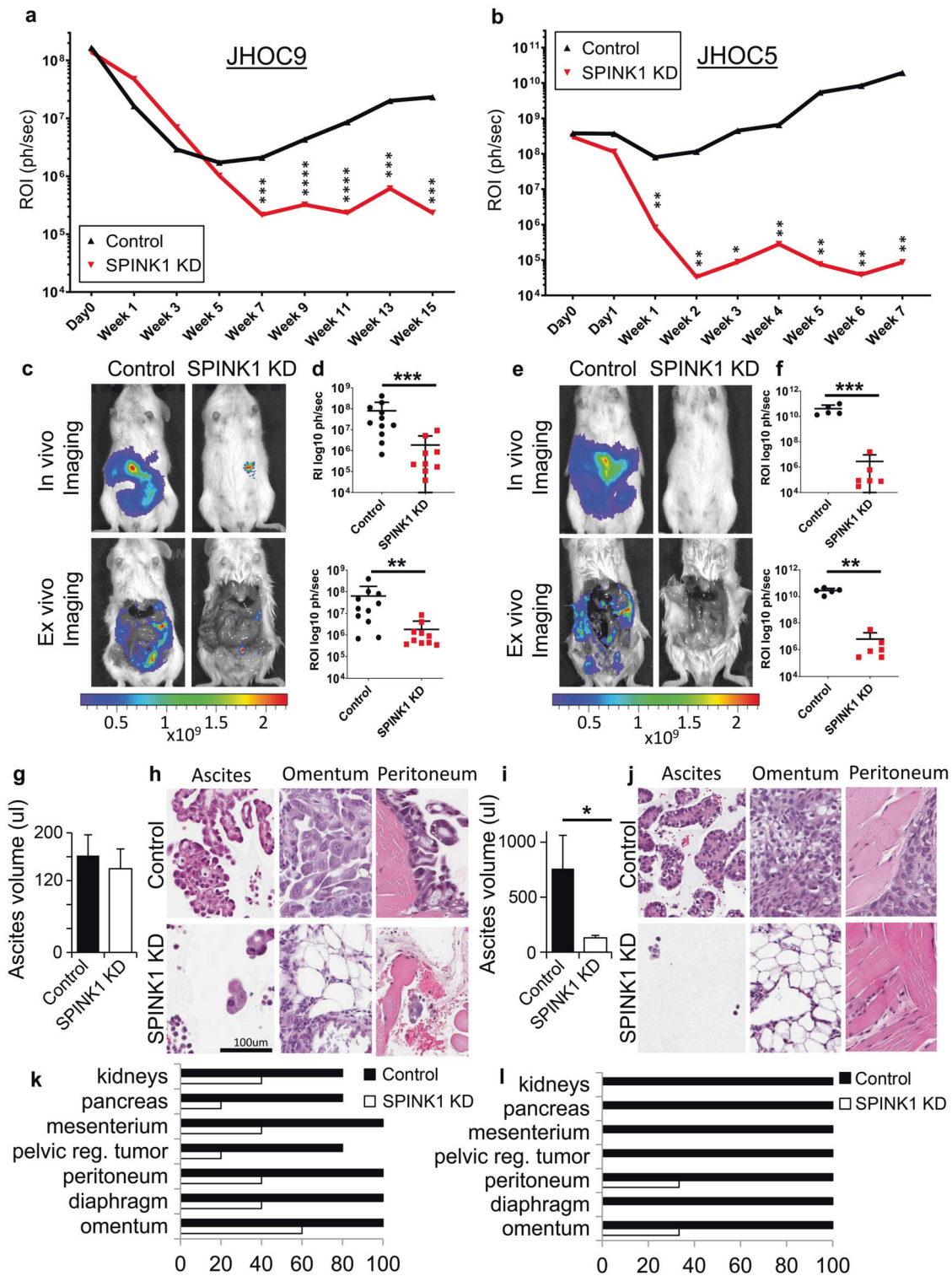
groups (Fig. 2h, j top left panels), while no tumor spheroids were found in either of the SPINK1 KD groups (Fig. 2h, j bottom left panels). IHC analysis also revealed reduced metastatic growth with SPINK1 knockdown for both cell lines in the omentum and peritoneum (Fig. 2h, j bottom middle and right panels), and SPINK1 knockdown also reduced tumor spread to the kidneys, pancreas, mesenterium, pelvic region, and diaphragm (Fig. 2k, l). These results demonstrate that SPINK1 expression is required for survival and metastasis of OCCC cell lines.

◄ **Fig. 2 SPINK1 knockdown in OCCC tumor cells reduces tumor burden and inhibits peritoneal metastasis.** Time course of tumor growth of JHOC9 (**a**) and JHOC5 (**b**) cells injected IP into NOD/SCID mice assessed using bioluminescent imaging revealed significantly reduced tumor burden from week 7 and beyond for JHOC9 SPINK1 KD as compared to nontarget control (NT, $n = 11$, KD, $n = 10$), and from week 1 and beyond for JHOC5 SPINK1 KD as compared to nontarget control (NT, $n = 5$, KD, $n = 6$). Reduced tumor spread with SPINK1 KD of JHOC9 (**c**, **d**) and JHOC5 (**e**, **f**) cells at time of harvest (JHOC9, 15 weeks; JHOC5, 7 weeks), assessed through in vivo imaging prior to harvest (**c**, **e** top; quantified in **d**, **f** top) and ex vivo imaging of the body cavity (**c**,**e** bottom; quantified in **d**, **f** bottom). Reduced acites volume (**g**, **i**) and reduced tumor presence in ascites and metastasis to omentum and peritoneum (**h**, **j**) with SPINK1 KD tumor mice for both JHOC9 (**g**, **h**) and JHOC5 (**i**, **j**) cells. Scoring extracted tissue for tumor cell presence (any size lesion) showed reduced presence in multiple organs with SPINK1 KD for both JHOC9 (**k**) and JHOC5 (**l**) tumor models. Mann–Whitney test *$p < 0.05$, **$p < 0.01$, ***$p < 0.001$.

IL-6 regulates gene expression of SPINK1 to promote anoikis resistance and proliferation of OCCC cells

The SPINK1 gene contains an IL-6 response element within the promoter region [19]; we therefore reasoned that IL-6 signaling might regulate SPINK1 expression by OCCC cells. Prior reports suggest that OCCC tumors and cell lines strongly express IL-6 and its receptor subunit gp130, whereas a subset also expresses receptor subunit IL-6Rα [23, 26]. To evaluate the potential for autocrine IL-6 signaling in our experimental models of OCCC, we assessed tumor staining for IL-6, IL-6Rα, and gp130 by IHC. We found staining for IL-6 and its receptor components in tumors from control mice bearing JHOC9 and JHOC5 tumors, and in a representative OCCC patient tumor (Fig. 3a–c). Notably, staining of adjacent tissue sections demonstrated colocalization of IL-6 and receptor components in tumor regions also positive for SPINK1 (Fig. 3a–c). Next, we silenced IL-6 expression in OCCC cells using lentiviral shRNA constructs (Fig. 3d), and found significant reduction in SPINK1 expression (Figs. 3e and S8), consistent with a regulatory role for IL-6. Conversely, cells treated for 48 h with recombinant IL-6 showed significantly elevated SPINK1 mRNA levels (Fig. 3f). Using an ELISA, we also determined SPINK1 protein levels in conditioned media from OCCC cells following shRNA knockdown of either SPINK1 or IL-6. Striking reduction in secreted SPINK1 by SPINK1 KD cells relative to control cells confirmed the efficacy of knockdown at the protein level, while significant reductions in secreted SPINK1 levels in the IL-6-KD cells further demonstrate the regulation of SPINK1 expression by IL-6 in these OCCC cell lines (Fig. 3g, h). Taken together, these results identify an autocrine signaling axis by which IL-6 regulates SPINK1 expression in OCCC cells.

To directly assess the impact of IL-6 on anoikis resistance, we next treated OCCC cells with recombinant IL-6 protein and plated them onto ultra-low attachment plates. IL-6 treatment led to a significant increase in cell survival in both cell lines compared to controls (Fig. 4a–c). Conversely, IL-6 knockdown (Fig. S9) led to significantly reduced cell survival under detached growth conditions in both cell lines (Fig. 4d–f), reproducing the effect of SPINK1 KD (Fig. 1a–c). Using a time course assay of anoikis, we found that the addition of recombinant SPINK1 could partially rescue the increased anoikis caused by IL-6 KD in both cell lines (Figs. 4g–h and S10). Further, we found that IL-6 KD significantly impaired proliferation compared to controls (Fig. 4i–k), again reproducing the effect of SPINK1 KD (Fig. 1f–h). Together, these results demonstrate that IL-6 promotes anoikis resistance and proliferation of OCCC cells at least in part through regulation of SPINK1 expression, identifying an IL-6–SPINK1 signaling axis that may offer plausible points of therapeutic intervention in OCCC.

SPINK1 and IL-6 are associated with a common protumorigenic expression profile in OCCC cells

To compare the overall impact of SPINK1 and IL-6 signaling in OCCC cells, we performed transcriptional profiling on JHOC9 and JHOC5 cells expressing nontarget control, SPINK1 KD, or IL-6 KD constructs. Comparison of SPINK1 KD samples to nontarget controls identified 2982 differentially expressed transcripts ($p < 0.05$), which mapped to 2081 genes. Comparison of publically available datasets with the SPINK1 KD dataset revealed significant overlap ($p = 3.0E − 16$) with comparison of OCCC vs. benign ovarian surface epithelium (Fig. 5a) [27] and six other ovarian cancer datasets (Fig. S11). Comparison of IL-6 KD samples to nontarget controls identified 2193 differentially expressed transcripts ($p < 0.05$), which mapped to 1343 genes. Comparison of the SPINK1 KD dataset and the IL-6 KD dataset identified 422 overlapping transcripts ($p = 3.0E − 55$, Fig. 5b) and broad overlap in gene expression patterns (Fig. 5c), including many genes involved in pathway regulation of proliferation and apoptotic pathways. Among these, we found that expression of BTG antiproliferation factor 2 (BTG2) is increased in SPINK1 KD and IL-6 KD cells (Fig. 5d, f); BTG2 is a tumor suppressor that suppresses proliferation and regulates apoptosis in multiple models [28]. By contrast, expression of riboflavin kinase (RFK), F-box protein 28 (FBXO28), and microtubule-associated serine/threonine kinase-like (MASTL) was found to be downregulated with both SPINK1 KD and IL-6 KD (Fig. 5e, g). RFK has been shown to correlate with resistance to cisplatin, while knockdown of the gene was shown to induce apoptosis in prostate cells [29]; FBXO28 overexpression has been linked to poor prognosis in breast cancer [30]; and MASTL has

Fig. 3 The IL-6 signaling pathway drives SPINK1 expression in OCCC. JHOC9 (**a**), JHOC5 (**b**), and human OCCC tumors (**c**) stained for SPINK1, IL-6, IL-6Rα, and gp130 in adjacent tissue sections demonstrated colocalization of SPINK1 expression with IL-6 pathway components (size bar = 100 μm). **d** JHOC9 cells transduced with lentiviral shRNA IL-6 knockdown constructs KD1 and KD2 showed significant reduction in IL-6 mRNA expression assessed by qRT/PCR. **e** Cells from **d** with knockdown of IL-6 also showed significant reduction of SPINK1 transcript expression (One-way Anova). **f** JHOC9 cells treated with 30 ng/ml recombinant human IL-6 for 48 h showed significantly increased SPINK1 transcript expression. Results assessed from triplicate wells (unpaired *t*-test). Conditioned media of JHOC9 cells (**g**) or JHOC5 cells (**h**) show significantly reduced SPINK1 protein concentration from cells transduced with SPINK1 or IL-6 knockdown constructs compared to nontarget control cells, as measured by ELISA. Results assessed in triplicate wells (One-way Anova). *$p < 0.05$, **$p < 0.01$, ***$p < 0.001$, ****$p < 0.0001$.
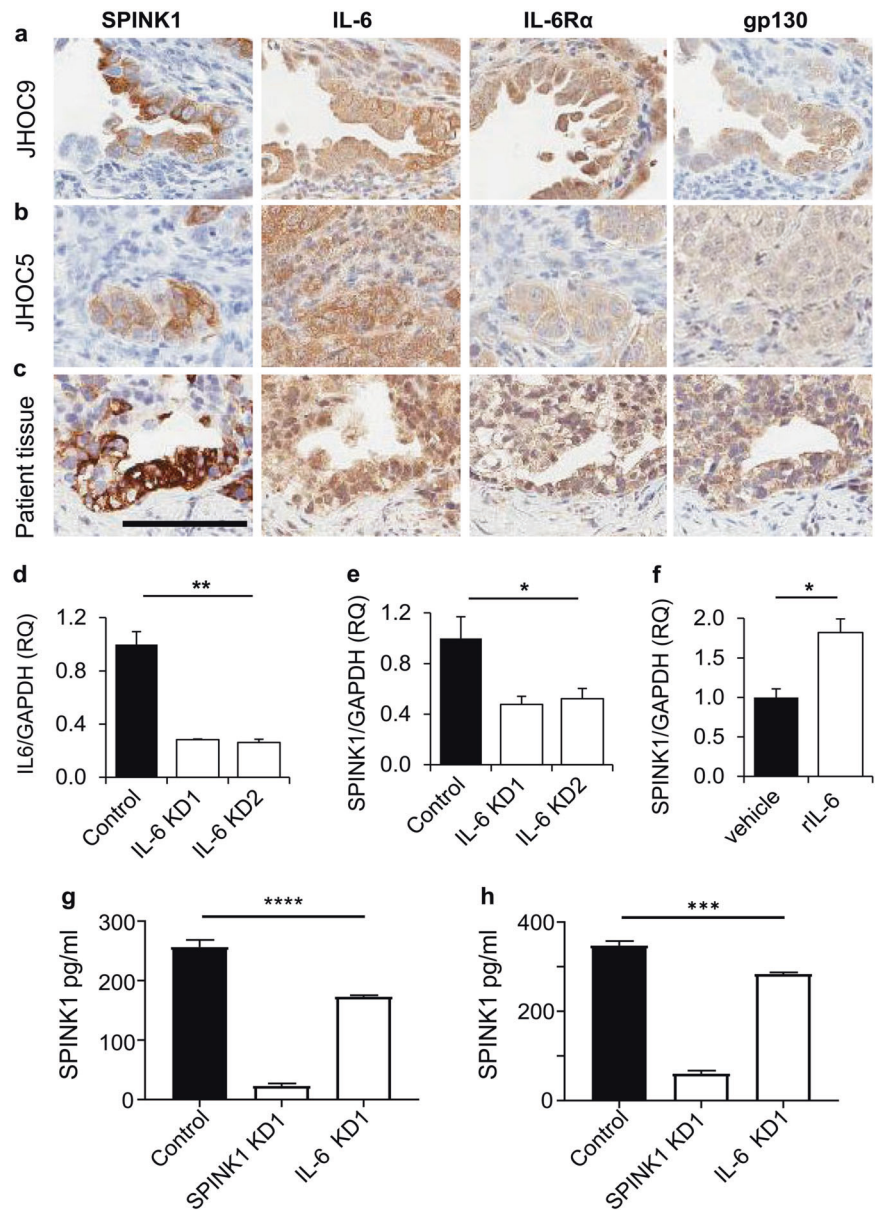
direct influence on major oncogenic pathways such as AKT/mTOR and Wnt/β-catenin [31]. These overlapping gene expression patterns further support an IL-6–SPINK1 signaling axis functioning to increase malignant potential in OCCC cancer cell lines.

IL-6Rα inhibitor tocilizumab reduces SPINK1-induced cell survival

Our studies implicating an IL-6–SPINK1 signaling axis in OCCC tumor cell proliferation and anoikis resistance suggested that pharmacological inhibition of IL-6 could have therapeutic benefit in OCCC. We tested the FDA-approved IL-6Rα inhibitor tocilizumab, which binds the IL-6Rα and thus inhibits the interaction between IL-6 and its membrane receptor, preventing downstream intracellular signaling. We found that tocilizumab treatment resulted in dose-dependent reductions of phosphorylation of STAT3 (pSTAT3, an IL-6 pathway target; Fig. 6a, b) and expression of SPINK1 (Fig. 6c). We also found that treatment reduced survival of cells cultured on ultra-low attachment plates, indicating bypass of SPINK1-induced anoikis resistance (Fig. 6d, e).

We next evaluated the efficacy of tocilizumab for inhibition of OCCC orthotopic tumor growth (Fig. 6f, j). We found significant reduction of ascites volume in the JHOC9 model with tocilizumab treatment (Fig. 6g), and a similar trend in the JHOC5 model (Fig. 6k), along with significantly reduced tumor metastasis to the diaphragm and omentum (Fig. 6h, i, l, m). Analysis of SPINK1 protein in ascites showed a trend toward reduced SPINK1 in tocilizumab-treated mice

Fig. 4 IL-6 increases tumor cell survival and tumor cell proliferation through SPINK1 expression. JHOC9 (**a**, **b**) and JHOC5 (**c**) cells treated with 30 ng/ml recombinant human IL-6 show significantly increased survival under attachment-free conditions. JHOC9 (**d**, **e**) and JHOC5 cells (**f**) with knockdown of IL-6 show significantly decreased survival relative to nontarget control cells under attachment-free conditions. Data shown represent the mean and SE of three independent experiments. (One-way Anova). Time course analysis of Annexin V binding to JHOC9 (**g**) and JHOC5 (**h**) cells with knockdown of IL-6 (green) and rescue of knockdown by addition of 500 nM recombinant SPINK1 (blue) as compared to nontarget control (black); quantification at 4 h time point. Data shown represent mean and SD for triplicate wells; these experiments were independently repeated with confirmatory results shown in Fig. S10 (unpaired *t*-test). Decreased proliferation was found in JHOC9 (**i**, **j**) and JHOC5 (**k**) cells with IL-6 knockdown relative to nontarget controls as assessed by EdU incorporation; data shown represent the mean and SE of two independent experiments (One-way Anova). *$p < 0.05$, **$p < 0.01$, ***$p < 0.001$.
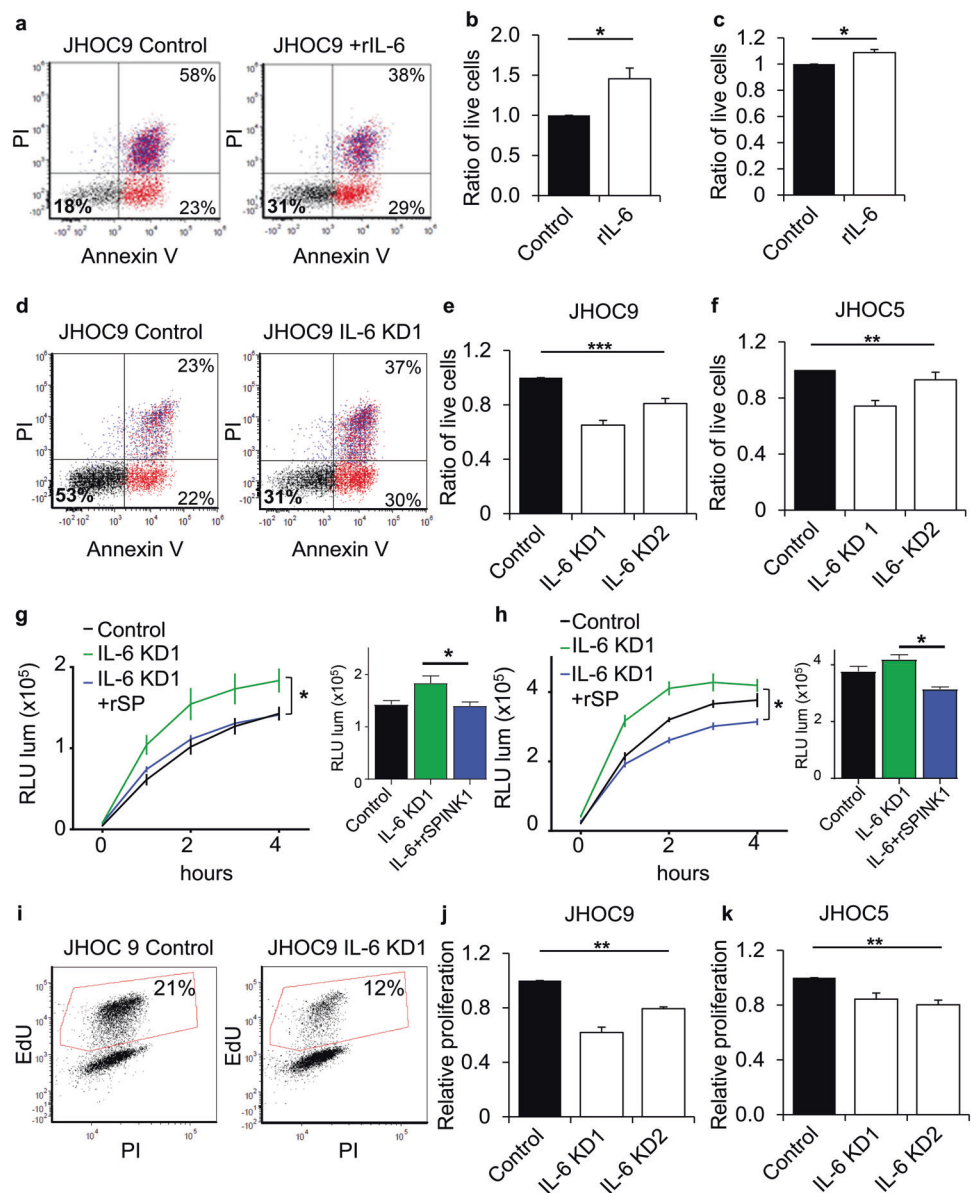
(Fig. S7b). These results demonstrate that the IL-6–SPINK1 signaling axis can be targeted pharmacologically, drastically reducing morbidity through reduction of ascites and overall tumor cell growth in abdominal metastatic lesions. Thus, targeting SPINK1-promoted growth and anoikis resistance through pharmacological inhibition of IL-6 could offer a promising approach for patients with OCCC tumors that show activation of this pathway.

Discussion

We define here an autocrine signaling axis in which OCCC tumor-cell-produced IL-6 induces SPINK1 to effect anoikis resistance and tumor cell proliferation. We further show that

this signaling axis can be therapeutically targeted by IL-6Rα inhibitors to significantly reduce ascites generation and tumor metastasis; these results strongly suggest that IL-6Rα inhibitors may be effective for treatment of OCCC patients with tumors expressing IL-6 and SPINK1.

SPINK1 detection in serum and immunostaining in tumor tissues have been identified as poor prognostic factors and potential biomarkers in multiple cancers, as described in recent review articles [13, 14, 32]. In prostate cancer, high levels of SPINK1 transcript or protein expression, present in about 10% of all prostate tumors, have been reported as an independent prognosticator for biochemical recurrence after resection [33]. High levels of SPINK1 immunostaining were also associated with poor survival in estrogen receptor positive breast cancers [34].
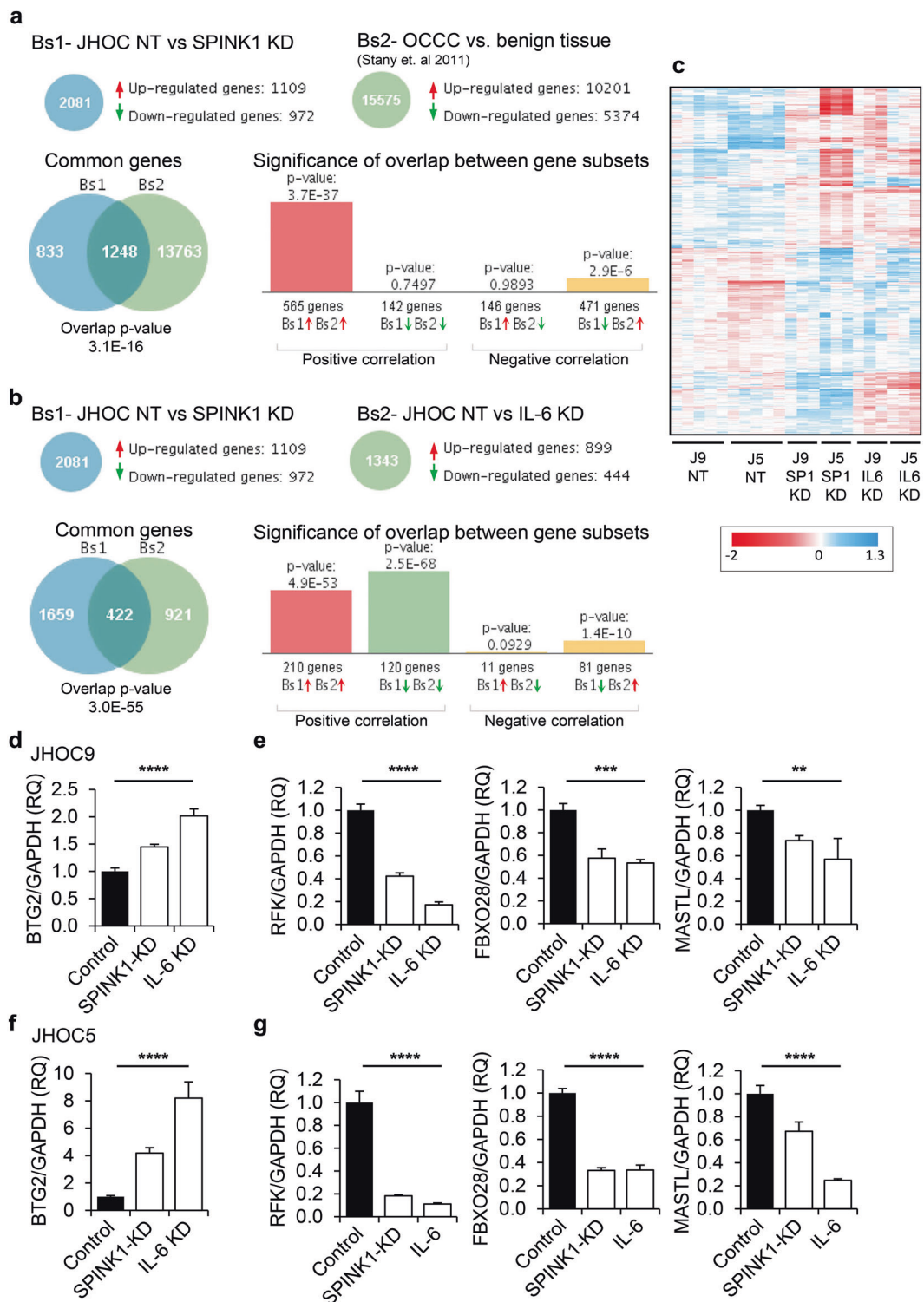
Fig. 5 Common gene expression patterns with knockdown of SPINK1 and IL-6. a Transcripts regulated by SPINK1 knockdown show significant overlap ($p = 3.0E - 16$) with dataset of ovarian clear cell carcinoma vs. benign tissue. **b** Transcripts regulated by SPINK1 knockdown and IL-6 knockdown show significant overlap ($p = 3.0E - 55$). **c** Heat map of 422 transcripts significantly regulated by SPINK1 knockdown and IL-6 knockdown (J9, JHOC9; J5, JHOC5; SP1 KD, SPINK1 knockdown; IL-6 KD, IL-6 knockdown). **d–g** Validation via qRT/PCR of common transcriptional alterations induced by SPINK1 knockdown and IL-6 knockdown. **d, f** BTG2 was consistently upregulated in both cell lines and in both SPINK1 KD and IL-6 KD. **e, g** RFK, FBXO28, and MASTL showed consistent reduced expression with both SPINK1 KD and IL-6 KD in both cell lines. qRT/PCR analysis was conducted in triplicate wells. One-way Anova $**p < 0.01$, $***p < 0.001$, $****p < 0.0001$.
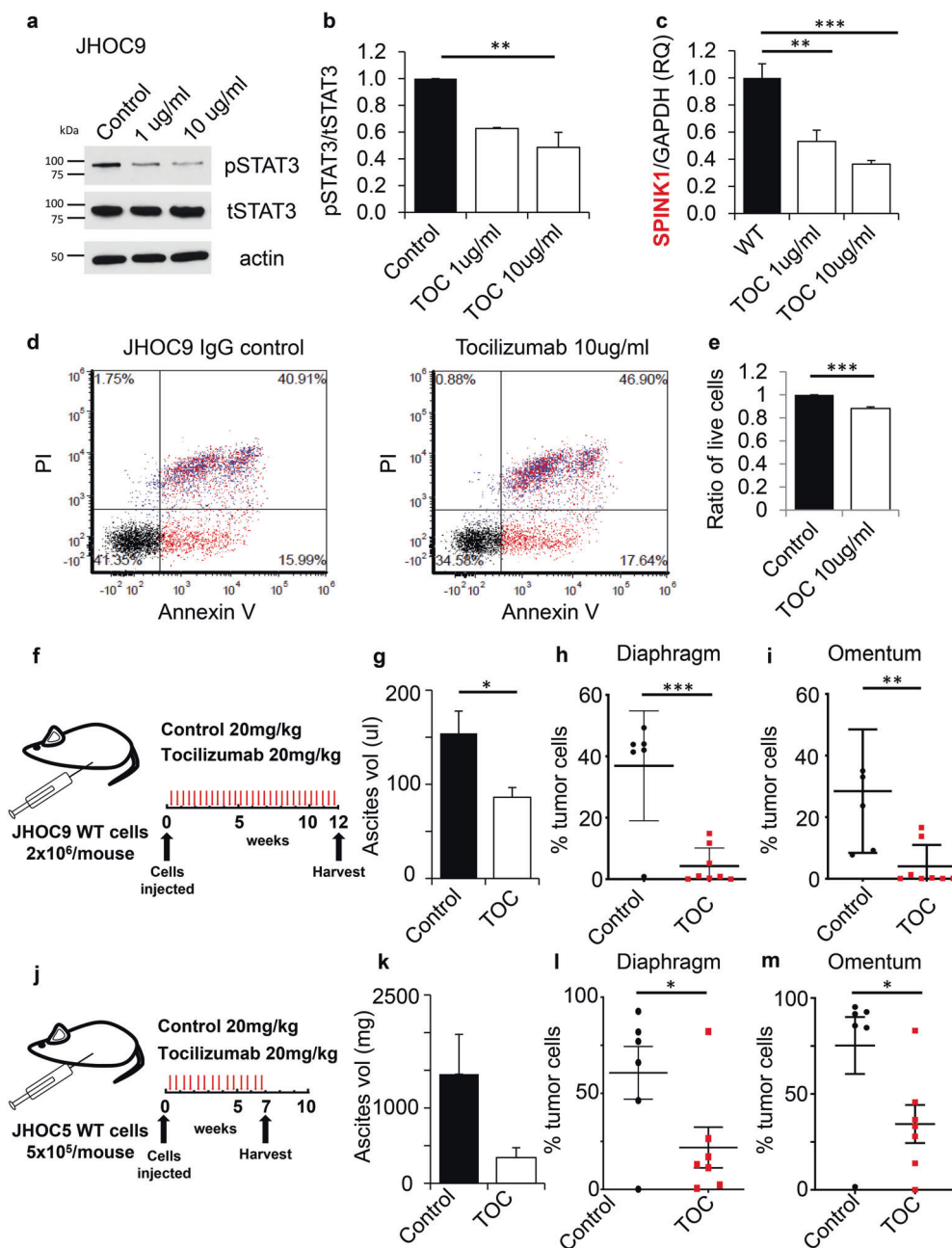
Fig. 6 Tocilizumab targets IL-6 signaling to reduce SPINK1 expression, tumor cell survival, ascites accumulation and metastasis. a, b JHOC9 cells treated for 48 h with tocilizumab, which targets IL-6Rα, showed decreased phosphorylation of downstream mediator STAT3 (**b**, quantification representing the mean and SE from two independent lysates, one-way Anova). **c** SPINK1 mRNA expression levels were significantly reduced after tocilizumab treatment (one-way Anova and unpaired *t*-test). **d, e** JHOC9 cells treated for 48 h with tocilizumab showed significantly reduced cell survival as assessed by Annexin V and PI staining (**e**, quantification represents the mean and SE of three independent experiments, unpaired *t*-test). Tocilizumab treatment of JHOC9 (**f–i**) and JHOC5 (**j–m**) tumor models resulted in decreased ascitic fluid (**g, k**) and reduced metastasis to diaphragm (**h, l**) and omentum (**i, m**), as compared to IgG control (unpaired *t*-test), **p < 0.01, ***p < 0.001.

Ovarian cancer is a particular area of interest, as increased SPINK1 levels have been detected in urine and cyst fluid of ovarian cancer patients, and SPINK1 has been investigated as a marker for early detection [35–37]. We have previously found that SPINK1 immunostaining in tumors represents an independent prognostic factor for poor survival, with strongest association in patients with nonserous histological tumor subtypes [11].

Investigations of tumor-promoting pathways activated by SPINK1 have furthermore demonstrated functional roles in cancer progression, implicating SPINK1 as a potential therapeutic target. These studies have identified mechanisms

associated with EGFR signaling and proliferation [14, 38], increased anoikis resistance [11], resistance to apoptosis [39, 40], and development of chemoresistance [34, 41]. In ovarian cancer, SPINK1 significantly impacts tumor cell proliferation and resistance to anoikis [11]. The present study adds to this knowledge by identifying the upstream regulator IL-6 as an essential driver of the SPINK1-induced phenotype specifically in OCCC, and defines this signaling axis as a promising target of therapeutic intervention.

OCCC is a unique disease, likely to be linked to pre-existing endometriosis, appearance of common mutations in ARID1A and PI3KCA, and is highly chemoresistant [6, 42, 43]. The current "one-size-fits-all" approach to treat ovarian cancer is underserving patients with OCCC, and new strategies are needed to target unique molecular drivers or vulnerabilities of OCCC. The IL-6–SPINK1 axis identified here presents a promising opportunity. Notably, we found consistent evidence for the significance of this pathway in two diverse models of OCCC, JHOC9 cells which possess ARID1A/PIK3CA mutations and JHOC5 cells which lack these mutations but possess high-level MET amplification, representative of a different subset of OCCCs [44]. Despite some broad differences between these cell lines evident in our transcriptional microarray studies, we found in common a protumorigenic transcriptional profile stimulated in both models by IL-6–SPINK1 signaling. Thus, our findings suggest that the IL-6–SPINK1 axis may be broadly relevant and of therapeutic interest across a range of OCCCs. Furthermore, targeting IL-6-mediated induction of SPINK1 allows the use of established therapeutics, as IL-6 inhibition has been the target of different drugs in previous clinical trials. While toxicity levels are low [45], phase-2 trials of the anti-IL-6 antibody siltuximab so far yielded disappointing results in unselected ovarian cancer patients [46, 47]. Given our preclinical results, however, it appears reasonable that such inhibitors may be more efficacious when targeted to OCCC patients with activated IL-6–SPINK1 pathways.

Current treatment includes early cytoreductive surgery, which is the most consistent method to increase survival and prolong time to recurrence [48]. However it cannot prevent the development or progression of malignant ascites and spread of abdominal metastasis. Metastasis is the leading cause for high morbidity and is a major contributor to mortality in ovarian cancer patients, with the majority of patients developing malignant ascites as part of their metastatic disease [9]. The occurrence of malignant ascites and abdominal metastasis is currently not preventable and only palliative measures of intervention are available [49, 50]. Our in vivo studies show that targeted treatment with an IL-6Rα inhibitor led to reduction of ascites volumes and reduced tumor cell proliferation and progression, suggesting that this treatment approach could reduce the ascites volumes and tumor burden in OCCC patients and increase their quality of life.

In summary we show that SPINK1 is a key player in anoikis resistance, proliferation, and development of metastatic lesions in OCCC. High levels of SPINK1 are driven by tumor-cell-expressed IL-6 through increased gene expression. The use of monoclonal antibodies against IL-6Rα significantly reduced SPINK1 expression and tumor cell survival in cell culture models, and in mouse models significantly reduced ascites volumes and the size of metastatic lesions in the abdominal cavity. Our work identifies a potential novel treatment option for a subset of OCCC patients with tumors expressing both IL-6 and SPINK1.

Materials and methods

Cells, reagents, and general methods

JHOC9 and JHOC5 cells were purchased from RIKEN BioResource Research Center (Ibaraki, Japan). Recombinant SPINK1 bearing a C-terminal 10×His-tag [51] was expressed from HEK293-FreeStyle cells following the protocol from Portolano et al. [52] and purified as previously described [11]. IL-6 recombinant protein was purchased from Sino Biological (Wayne, PA), resuspended in 0.1% BSA DPBS (stock 30 µg/ml), and aliquots stored at −20 °C. SPINK1/TATI PicoKine ELISA kit (#EK1241) was purchased from Boster Biological (Pleasanton, CA). Antibodies for Western blot were: pSTAT3—CST #9145; tSTAT3—CST #9139 (Cell Signaling Technologies, Danvers, MA); actin—SC #1616 (Santa Cruz Biotechnology, Dallas, TX). Antibodies for IHC were: SPINK1—4D4, H00006690-M01 (Novus Biologicals, Centennial, CO), IL-6—ab9324 (Abcam, Cambridge, UK), IL-6Rα—#B6362 (LS Bio, Seattle, WA), and gp130—#HPA010558 (Sigma, St Louis, MO). Details of cell culture, lentiviral knockdown, quantitative real-time PCR, Western blot, and ELISA procedures are described in the Supplementary Materials and Methods.

Anoikis resistance assay

For flow cytometry-quantified anoikis resistance assays, 1×10^5 cells were plated in serum-free media in six-well ultra-low attachment plates to observe anoikis. JHOC9 cells were then incubated for 10 h and JHOC5 for 4 h (positive control: staurosporine). Thereafter, cells were harvested, and apoptosis was determined using the Apoptosis Kit including Annexin V Alexa Fluor 488 and propidium iodide (PI) (V13241, Thermo Fisher) following the manufacturer's protocol. Briefly, cells were washed with PBS, and incubated for 15 min at room temperature with Annexin V/PI. Samples were analyzed using the Attune NxT flow

cytometer (lasers: BL1, YL1). Samples were gated for positivity for both Annexin V binding and PI integration. Analysis was performed using FCS Express 5, determining ratio of live cells. All experiments reported represent three biological replicates, with quantification displayed in bar graphs representing the average and standard error of the mean for the three independent experiments. For plate-reader-quantified anoikis resistance assays, 5×10^3 cells (JHCO9, JHOC5) were plated in complete media in luminescence supporting 96-well plates and recombinant proteins were added where applicable. Each condition was repeated in triplicate wells. RealTimeGlo Apoptosis and Necrosis Assay (#JA1011, Promega) was added according to the manufacturer's protocol. Resistance to cell death was determined over a time course via luminescence (apoptosis signal) using a plate reader (Veritas, Turner BioSystems). Data were analyzed using GraphPad Prism 8.0.

EdU proliferation assay

The 5-ethynyl-2′-deoxyuridine (EdU) incorporation assay was used to determine the amount of cells actively undergoing DNA synthesis. JHOC9 and JHOC5 cells (1×10^5), subjected to shRNA knockdown of SPINK1 or IL-6, were seeded in six-well plates and cultured in complete media for 18 h at 37 °C and humidified atmosphere with 5% CO_2. Fresh, pre-equilibrated complete media containing EdU was added to the cells for 2 h for incorporation. Subsequent washes and staining were performed following the manufacturer's instruction for the Click-iT EdU Alexa Fluor 488 kit (C10632, Thermo Fisher). Fixed and permeabilized cells were treated with Click-iT reaction cocktail, counter stained with PI for visualization, and analyzed using the Attune NxT flow cytometer. All experiments shown represent two biological replicates, with quantification displayed in bar graphs representing the average and standard error of the mean for the two independent experiments. Data analysis was performed using FCS Express 5.

Tocilizumab studies

To determine effects of tocilizumab on SPINK1 mRNA expression, cells (1×10^5) were plated in a six-well plate overnight followed by treatment with tocilizumab (1 and 10 µg/ml) for 48 h. Cells were washed, and RNA isolated using the TRIzol method and analyzed by qRT/PCR for SPINK1 as above. To assess tocilizumab effect on cell survival, cells (1×10^5) were seeded in a six-well plate, cultured overnight, and treated with tocilizumab for 48 h. Cells were then transferred onto six-well ultra-low attachment plates for 10 h before staining with Annexin V and PI as described above. All experiments were repeated in three independent biological replicates; analyses reflect the

pooled results, mean + SE. Data were analyzed using GraphPad Prism 8.0.

Microarray

RNA from three independent SPINK1 KD experiments with nontarget controls and from three independent IL-6 KD experiments with nontarget controls were extracted using TRIzol (Invitrogen) and evaluated for differences in gene expression using the Affymetrix human transcriptome Array v2.0. Results were analyzed using GeneSpring 14.9.1 (Agilent), as described previously [53, 54]. Briefly, data were processed using GCRMA and filtered to remove entities (transcripts) with raw data values below 50 in more than 75% of the samples, and moderated t-tests were used to identify differentially expressed entities when comparing knockdown samples (combining all JHOC9 and JHOC5 knockdown samples) vs. controls (combining all JHOC9 and JHOC5 nontarget control samples), which were mapped to genes and compared as genesets to publically available databases using Illumina Correlation Engine. Gene expression profiles have been deposited in the Gene Expression Omnibus (GSE140179).

Animal models and bioluminescence imaging

Animal studies were conducted in accordance with the guidelines and approval by the Mayo Clinic Institutional Animal Care and Use Committee (protocol A00002844-17). This study used 6–8-week-old female Nod/SCID mice for tumor cell injection; mice were distributed among experimental groups so as to achieve a similar age distribution within each group. Studies including SPINK1 KD used lentiviral shRNA-transduced cells that were subsequently transduced with luciferase lentivirus for in vivo imaging. Knockdown efficiency was confirmed by qRT/PCR (Fig. S5a, b). Imaging of titrated cells (see Supplementary Materials and Methods) taken immediately prior to injection showed equal intensity of bioluminescence for all experimental conditions (Fig. S6a, b). JHOC9 cells (2×10^6) or JHOC5 cells (5×10^5) transduced with either NT (control) or SPINK1 KD virus were injected IP into the lower right quadrant of the abdomen. Cell injection was followed by luciferin IP injection (150 mg/kg of D-luciferin) and then mice were imaged for bioluminescent signal after 8 min (IVIS Spectrum 3D imaging system, Caliper Life Sciences). JHOC9 cohorts were euthanized at 15 weeks, and JHOC5 cohorts at 7 weeks due to tumor growth kinetics and moribund endpoints. Mice in studies investigating the impact of IL-6 inhibitor tocilizumab received 2×10^6 JHOC9 or 5×10^5 JHOC5 cells transduced with luciferase lentivirus. After 24 h mice were assigned to treatment or control groups, such that distribution of day 1 pre-treatment luciferase imaging signal

intensity was comparable between groups. Subsequently, the treatment group received tocilizumab 20 mg/kg (Actemra, Genentech), and the control group received IgG control 20 mg/kg (Jackson ImmunoResearch, West Grove, PA). Treatment and control mice were injected every 48 h (JHOC9) or every 72 h (JHOC5) IP. Mice were imaged weekly to monitor tumor cell development and expansion, and were subsequently euthanized at 12 weeks (JHOC9) or 7 weeks (JHOC5). For all mouse experiments, the bioluminescent signal was imaged and quantified by EM and analyzed by CM. Immediately before harvest, mice were injected with luciferase as above and a final in vivo image obtained. Mice were then euthanized by CO_2 asphyxiation. Ascitic fluid was retrieved from the abdominal cavity and quantified. Evaluation of ascitic fluid was conducted in a manner blinded to the investigator. The opened body cavity was imaged ex vivo for detection of bioluminescent signal. Tissues were then formalin-fixed and embedded for IHC. Ascitic fluid was centrifuged to pellet the cellular component. Cells contained in the ascitic fluid were formalin-fixed and embedded into histogel (VWR, Thermo Scientific) followed by paraffin embedding for IHC. Power calculations are detailed in Supplementary Materials and Methods.

Compliance with ethical standards

Conflict of interest The authors declare that they have no conflict of interest.

Publisher's note Springer Nature remains neutral with regard to jurisdictional claims in published maps and institutional affiliations.

References

1. Howlader N, Noone AM, Krapcho M, Miller D, Brest A, Yu M, et al. SEER cancer statistics review, 1975–2016. Bethesda, MD: National Cancer Institute; 2017.
2. Lengyel E. Ovarian Cancer Development and Metastasis. Am J Pathol. 2010;177:1053–64.
3. Mitra AK. Ovarian cancer metastasis: a unique mechanism of dissemination. In: Xu K (editor). Tumor metastasis. Rijeka: InTech; 2016.
4. du Bois A, Lück H-J, Meier W, Adams H-P, Möbus V, Costa S, et al. A randomized clinical trial of cisplatin/paclitaxel versus carboplatin/paclitaxel as first-line treatment of ovarian cancer. J Natl Cancer Inst. 2003;95:1320–9.
5. Sugiyama T, Kamura T, Kigawa J, Terakawa N, Kikuchi Y, Kita T, et al. Clinical characteristics of clear cell carcinoma of the ovary: a distinct histologic type with poor prognosis and resistance to platinum-based chemotherapy. Cancer. 2000;88:2584–9.
6. Takano M, Kikuchi Y, Yaegashi N. Clear cell carcinoma of the ovary: a retrospective multicentre experience of 254 patients with complete surgical staging. Br J Cancer. 2006;94:1369–74.
7. del Carmen MG, Birrer M, Schorge JO. Clear cell carcinoma of the ovary: a review of the literature. Gynecologic Oncol. 2012;126:481–90.
8. Chan JK, Teoh D, Hu JM, Shin JY, Osann K, Kapp DS. Do clear cell ovarian carcinomas have poorer prognosis compared to other epithelial cell types? A study of 1411 clear cell ovarian cancers. Gynecologic Oncol. 2008;109:370–6.
9. Ahmed N, Stenvers KL. Getting to know ovarian cancer ascites: opportunities for targeted therapy-based translational research. Front Oncol. 2013;3:256.
10. Simpson CD, Anyiwe K, Schimmer AD. Anoikis resistance and tumor metastasis. Cancer Lett. 2008;272:177–85.
11. Mehner C, Oberg AL, Kalli KR, Nassar A, Hockla A, Pendlebury D, et al. Serine protease inhibitor Kazal type 1 (SPINK1) drives proliferation and anoikis resistance in a subset of ovarian cancers. Oncotarget. 2015;6:35737–54.
12. Rinderknecht H. Activation of pancreatic zymogens. Normal activation, premature intrapancreatic activation, protective mechanisms against inappropriate activation. Dig Dis Sci (Rev). 1986;31:314–21.
13. Itkonen O, Stenman UH. TATI as a biomarker. Clin Chim Acta; Int J Clin Chem. 2014;431:260–9.
14. Rasanen K, Itkonen O, Koistinen H, Stenman UH. Emerging roles of SPINK1 in cancer. Clin Chem. 2016;62:449–57.
15. Stenman UH. Role of the tumor-associated trypsin inhibitor SPINK1 in cancer development. Asian J Androl. 2011;13:628–9.
16. Hunter CA, Jones SA. IL-6 as a keystone cytokine in health and disease. Nat Immunol (Rev). 2015;16:448–57.
17. Taniguchi K, Karin M. IL-6 and related cytokines as the critical lynchpins between inflammation and cancer. Semin Immunol. 2014;26:54–74.
18. Yasuda T, Ogawa M, Murata A, Oka Y, Uda K, Mori T. Response to IL-6 stimulation of human hepatoblastoma cells: production of pancreatic secretory trypsin inhibitor. Biol Chem Hoppe Seyler. 1990;371(Suppl):95–100.
19. Yasuda T, Ogawa M, Murata A, Ohmachi Y, Yasuda T, Mori T, et al. Identification of the IL-6-responsive element in an acute-phase-responsive human pancreatic secretory trypsin inhibitor-encoding gene. Gene. 1993;131:275–80.
20. Rasanen K, Lehtinen E, Nokelainen K, Kuopio T, Hautala L, Itkonen O, et al. Interleukin-6 increases expression of serine protease inhibitor Kazal type 1 through STAT3 in colorectal adenocarcinoma. Mol Carcinog. 2016;55:2010–23.
21. Watson JM, Sensintaffar JL, Berek JS, Martinez-Maza O. Constitutive production of interleukin 6 by ovarian cancer cell lines and by primary ovarian tumor cultures. Cancer Res. 1990;50:6959–65.
22. Nilsson MB, Langley RR, Fidler IJ. Interleukin-6, secreted by human ovarian carcinoma cells, is a potent proangiogenic cytokine. Cancer Res. 2005;65:10794–800.
23. Anglesio MS, George J, Kulbe H, Friedlander M, Rischin D, Lemech C, et al. IL6-STAT3-HIF signaling and therapeutic response to the angiogenesis inhibitor sunitinib in ovarian clear cell cancer. Clin Cancer Res. 2011;17:2538–48.
24. Chandler RL, Damrauer JS, Raab JR, Schisler JC, Wilkerson MD, Didion JP, et al. Coexistent ARID1A–PIK3CA mutations promote

ovarian clear-cell tumorigenesis through pro-tumorigenic inflammatory cytokine signalling. Nat Commun. 2015;6:6118.

25. Kawabata A, Yanaihara N, Nagata C, Saito M, Noguchi D, Takenaka M, et al. Prognostic impact of interleukin-6 expression in stage I ovarian clear cell carcinoma. Gynecologic Oncol. 2017;146:609–14.

26. Yanaihara N, Hirata Y, Yamaguchi N, Noguchi Y, Saito M, Nagata C, et al. Antitumor effects of interleukin-6 (IL-6)/interleukin-6 receptor (IL-6R) signaling pathway inhibition in clear cell carcinoma of the ovary. Mol Carcinog. 2016;55:832–41.

27. Stany MP, Vathipadiekal V, Ozbun L, Stone RL, Mok SC, Xue H, et al. Identification of novel therapeutic targets in microdissected clear cell ovarian cancers. PLoS ONE. 2011;6:e21121.

28. Yuniati L, Scheijen B, van der Meer LT, van Leeuwen FN. Tumor suppressors BTG1 and BTG2: Beyond growth control. J Cell Physiol. 2019;234:5379–89.

29. Hirano G, Izumi H, Yasuniwa Y, Shimajiri S, Ke-Yong W, Sasagiri Y, et al. Involvement of riboflavin kinase expression in cellular sensitivity against cisplatin. Int J Oncol. 2011;38:893–902.

30. Cepeda D, Ng HF, Sharifi HR, Mahmoudi S, Cerrato VS, Fredlund E, et al. CDK-mediated activation of the SCF(FBXO) (28) ubiquitin ligase promotes MYC-driven transcription and tumourigenesis and predicts poor survival in breast cancer. EMBO Mol Med. 2013;5:1067–86.

31. Marzec K, Burgess A. The oncogenic functions of MASTL kinase. Front Cell Dev Biol. 2018;6:162

32. Stenman U-H. Tumor-associated trypsin inhibitor. Clin Chem. 2002;48:1206–9.

33. Tomlins SA, Rhodes DR, Yu J, Varambally S, Mehra R, Perner S, et al. The role of SPINK1 in ETS rearrangement-negative prostate cancers. Cancer Cell. 2008;13:519–28.

34. Soon WW, Miller LD, Black MA, Dalmasso C, Chan XB, Pang B, et al. Combined genomic and phenotype screening reveals secretory factor SPINK1 as an invasion and survival factor associated with patient prognosis in breast cancer. EMBO Mol Med. 2011;3:451–64.

35. Halila H, Huhtala ML, Haglund C, Nordling S, Stenman UH. Tumour-associated trypsin inhibitor (TATI) in human ovarian cyst fluid. Comparison with CA 125 and CEA. Br J Cancer. 1987;56:153–6.

36. Huhtala ML, Pesonen K, Kalkkinen N, Stenman UH. Purification and characterization of a tumor-associated trypsin inhibitor from the urine of a patient with ovarian cancer. J Biol Chem. 1982;257:13713–6.

37. Paju A, Vartiainen J, Haglund C, Itkonen O, von Boguslawski K, Leminen A, et al. Expression of trypsinogen-1, trypsinogen-2, and tumor-associated trypsin inhibitor in ovarian cancer: prognostic study on tissue and serum. Clin Cancer Res. 2004;10:4761–8.

38. Ateeq B, Tomlins SA, Laxman B, Asangani IA, Cao Q, Cao X, et al. Therapeutic targeting of SPINK1-positive prostate cancer. Sci Transl Med. 2011;3:72ra17.

39. Lamontagne J, Pinkerton M, Block TM, Lu X, Hepatitis B, Hepatitis C. Virus replication upregulates serine protease inhibitor Kazal, resulting in cellular resistance to serine protease-dependent apoptosis. J Virol. 2010;84:907–17.

40. Lu X, Lamontagne J, Lu F, Block TM. Tumor-associated protein SPIK/TATI suppresses serine protease dependent cell apoptosis. Apoptosis: Int J Program Cell Death. 2008;13:483–94.

41. Chen F, Long Q, Fu D, Zhu D, Ji Y, Han L, et al. Targeting SPINK1 in the damaged tumour microenvironment alleviates therapeutic resistance. Nat Commun. 2018;9:4315.

42. Wiegand KC, Shah SP, Al-Agha OM, Zhao Y, Tse K, Zeng T, et al. ARID1A mutations in endometriosis-associated ovarian carcinomas. N Engl J Med. 2010;363:1532–43.

43. Sugiyama T, Yakushiji M, Nishida T. Irinotecan (CPT-11) combined with cisplatin in patients with refractory or recurrent ovarian cancer. Cancer Lett. 1998;128:211–8.

44. Anglesio MS, Wiegand KC, Melnyk N, Chow C, Salamanca C, Prentice LM, et al. Type-specific cell line models for type-specific ovarian cancer research. PLoS ONE. 2013;8:e72162.

45. Dijkgraaf EM, Santegoets SJ, Reyners AK, Goedemans R, Wouters MC, Kenter GG, et al. A phase I trial combining carboplatin/doxorubicin with tocilizumab, an anti-IL-6R monoclonal antibody, and interferon-alpha2b in patients with recurrent epithelial ovarian cancer. Ann Oncol: Off J Eur Soc Med Oncol. 2015;26:2141–9.

46. Coward J, Kulbe H, Chakravarty P, Leader D, Vassileva V, Leinster DA, et al. Interleukin-6 as a therapeutic target in human ovarian cancer. Clin Cancer Res. 2011;17:6083–96.

47. Angevin E, Tabernero J, Elez E, Cohen SJ, Bahleda R, van Laethem JL, et al. A phase I/II, multiple-dose, dose-escalation study of siltuximab, an anti-interleukin-6 monoclonal antibody, in patients with advanced solid tumors. Clin Cancer Res. 2014;20:2192–204.

48. Pectasides D, Pectasides E, Psyrri A, Economopoulos T. Treatment issues in clear cell carcinoma of the ovary: a different entity? oncologist. 2006;11:1089–94.

49. Kipps E, Tan DS, Kaye SB. Meeting the challenge of ascites in ovarian cancer: new avenues for therapy and research. Nat Rev Cancer. 2013;13:273–82.

50. Al-Quteimat OM, Al-Badaineh MA. Intraperitoneal chemotherapy: rationale, applications, and limitations. J Oncol Pharm Pract: Off Publ Int Soc Oncol Pharm Pract. 2014;20:369–80.

51. Kereszturi E, Kiraly O, Sahin-Toth M. Minigene analysis of intronic variants in common SPINK1 haplotypes associated with chronic pancreatitis. Gut. 2009;58:545–9.

52. Portolano N, Watson PJ, Fairall L, Millard CJ, Milano CP, Song Y, et al. Recombinant protein expression for structural biology in HEK 293F suspension cells: a novel and accessible approach. J Vis Exp. 2014;92:e51897.

53. Cichon MA, Nelson CM, Radisky DC. Regulation of epithelial-mesenchymal transition in breast cancer cells by cell contact and adhesion. Cancer Inf. 2015;14:1–13.

54. Ma H, Hockla A, Mehner C, Coban M, Papo N, Radisky DC, et al. PRSS3/Mesotrypsin and kallikrein-related peptidase 5 are associated with poor prognosis and contribute to tumor cell invasion and growth in lung adenocarcinoma. Sci Rep. 2019;9:1844.